01 Apr 2023

Performance Assessment of Bioasphalt Mixtures Containing Guayule Resin as an Innovative Biobased Asphalt Alternative

Ahmed Hemida

Magdy Abdelrahman
Missouri University of Science and Technology, abdelrahmanm@mst.edu

Performance Assessment of Bioasphalt Mixtures Containing Guayule Resin as an Innovative Biobased Asphalt Alternative

Ahmed Hemida, Ph.D., Aff.M.ASCE[1]; and Magdy Abdelrahman, Ph.D., A.M.ASCE[2]

Abstract: Guayule resin was investigated through mixture to assess its role in the field performance. For performance comparisons, conventional asphalt, neat guayule, asphalt–rubber–guayule, and guayule–rubber binders were implied. Field-simulated lab mixtures were made to investigate the major distresses. Modified Lottman, rut, semicircular bending, and disk-shaped compact tension tests were used to assess stripping, rutting, fatigue, and thermal cracking resistances. Stripping and rutting susceptibilities were also assessed by Hamburg wheel-tracking test. The outcomes disclosed that when the modified Lottman test was used, guayule containing a 7% air content was more susceptible to stripping than that containing a 3.5% air content, resulting in tensile strength ratios of 40% and 71%, respectively. All investigated mixtures did not reach out the stripping inflection point under the Hamburg wheel-tracking criteria. Asphalt offered the worst Hamburg rut depth, which was 3.2 mm after 20,000 passes. Guayule-based mixtures perfectly resisted rutting as proven by the rut test. Guayule offered the worst rut depth of 6.3 mm, indicating a great rutting resistance. The guayule-based mixture had a high fracture toughness at intermediate temperatures. Guayule and guayule–rubber mixtures offered a critical strain energy release rate of 0.65–0.69 kJ/m^2 compared to 0.46 kJ/m^2 for asphalt. They, however, tended to possess low thermal fracture resistance (less than the threshold fracture energy, 400 J/m^2). Conversely, a blend of 62.5% asphalt, 12.5% rubber, and 25% guayule offered 591 J/m^2 at its performance grade low temperature (−16°C) and 409 J/m^2 at −22°C compared to 429 J/m^2 for asphalt at the later temperature, which represented the performance-grade low temperature of asphalt.
DOI: 10.1061/(ASCE)MT.1943-5533.0004682.

Author keywords: Bioasphalt; Guayule resin; Hot mix asphalt; Performance testing; Sustainability.

Introduction

Guayule resin is inherently extracted during the production of guayule natural rubber (current target guayule product) in the same proportion of 1:1, at the very least (Nakayama 2005). Guayule resin is a by-product (leftover) (Nakayama 2005; Rasutis et al. 2015), but it has the potential to become an asphalt cement alternative (Hemida and Abdelrahman 2018, 2019a, 2020a, b, 2021a, b, c). Hemida and Abdelrahman in these later references investigated the guayule resin's applicability from the perspective of binder performance. It is an asphalt-like material (Hemida and Abdelrahman 2021c). It provides rheological properties comparable to asphalt cement, thermoplastic viscoelastic, and susceptible to temperature changes (viscoelastic at room temperature, liquid at high temperatures, and solid at low temperatures) (Hemida and Abdelrahman 2021c). Therefore, the guayule-based binder could represent an innovative approach to replace asphalt cement for a sustainable, flexible pavement industry (Hemida and Abdelrahman 2021b, c).

Several bio-oils were investigated in literature for asphalt binder replacement (Hemida and Abdelrahman 2019b). The distinction of guayule resin is that it is readily usable in the massive, flexible pavement industry. The only process needed is a simple heat treatment to ensure that no moisture and/or low molecular weight components are inside before further processing (Hemida and Abdelrahman 2020b). Nevertheless, guayule resin is not identical to asphalt cement (Hemida and Abdelrahman 2021a). Guayule resin offered a lower viscosity for the construction process than conventional asphalt at the same performance grade high temperature (PG-HT) (Hemida and Abdelrahman 2021b). This could indicate plant energy consumption and environmental emissions savings (Hemida and Abdelrahman 2021b). According to the literature, the as-received guayule resin could provide a PG-HT of up to 58°C (Hemida and Abdelrahman 2021a) and a performance grade low temperature (PG-LT) of −16°C (Hemida and Abdelrahman 2021b). These performance grades are not widely applicable in several locations (Hemida and Abdelrahman 2021a). Therefore, guayule modifications potentially enhance the guayule-based binder's performance. For instance, it was proved that the crumb rubber modifier (CRM or rubber) improved the PG-HT of the neat guayule (Hemida and Abdelrahman 2021a, b). However, CRM did not enhance its PG-LT (Hemida and Abdelrahman 2021b). Nothing enhanced the guayule-based binder's PG-LT except for the partial asphalt replacement by guayule (Hemida and Abdelrahman 2021a, b). Rejuvenators could be used in the future to enhance the PG-LT of the guayule-based binders. Put simply, asphalt cement performance was enhanced via many years of research, and guayule has the potential to achieve a wide tolerance of high- and low-temperature performance grades by future investigations.

[1]Assistant Professor, Dept. of Construction & Building Engineering, Arab Academy for Science, Technology and Maritime Transport, P.O. Box 1029, Alexandria, Egypt (corresponding author). ORCID: https://orcid.org/0000-0002-8651-5536. Email: a.hemida@aast.edu

[2]Missouri Asphalt Pavement Association (MAPA) Endowed Professor, Dept. of Civil, Architectural, and Environmental Engineering, Missouri Univ. of Science and Technology, Rolla, MO 65409. Email: m.abdelrahman@mst.edu

Note. This manuscript was submitted on December 23, 2021; approved on July 14, 2022; published online on January 20, 2023. Discussion period open until June 20, 2023; separate discussions must be submitted for individual papers. This paper is part of the ***Journal of Materials in Civil Engineering***, © ASCE, ISSN 0899-1561.

The literature stated that CRM significantly enhanced the conventional asphalt's rheological properties (Deef-Allah et al. 2020). However, the harmony of the asphalt–rubber blend was higher than that of the guayule–rubber blend (Hemida and Abdelrahman 2021b). For instance, at high temperatures, it was found that 20% of CRM (by weight of asphalt) enhanced the neat asphalt by about three grades, and the same CRM concentration enhanced the neat guayule by only one grade (Hemida and Abdelrahman 2021b). Therefore, applying a blend of asphalt, rubber, and guayule resin as a partial asphalt cement replacement could yield a competitive performance against conventional asphalts at high-, intermediate-, and low-temperature performances (Hemida and Abdelrahman 2019a, 2021a, b).

Major distresses of asphalt mixtures were evaluated by several methods, including permanent deformation (rutting), load-associated (fatigue) cracking, low-temperature (thermal) cracking, and moisture susceptibility (FHWA 2013). Superpave mix design recognized the modified Lottman test to assess the mixture's moisture susceptibility (Roberts et al. 1996). Even though researchers used this standard method, there is a belief that it is not highly correlated to the field performance (Rafiq et al. 2020). Therefore, the Hamburg wheel tracking (HWT) test is commonly used to provide a high correlation with the actual performance and provide the rutting assessment by measuring rut depth (ASTM 2016; Rafiq et al. 2020). Researchers used fracture mechanics to evaluate fracture cracking at intermediate (fatigue cracking) and low (thermal cracking) temperatures (Radeef et al. 2021). Simply, fracture energy represented the energy required to form a new fracture surface (Radeef et al. 2021). This kind of testing is based on initiating a notch to control the crack propagation direction (Ahmad et al. 2020). Two of the most commonly used fracture resistance tests to evaluate the mixture cracking are the semi-circular bending (SCB) and disk-shaped compact tension (DCT) tests. The SCB test is used to assess the fatigue fracture resistance (Ahmad et al. 2020). The DCT test is one of the most recommended tests to evaluate the mixture thermal cracking (Stempihar 2013; Stewart et al. 2017), which has an adequate cracking path due to its relatively long cracking path compared to other tests (e.g., SCB test at low temperatures) (Radeef et al. 2021; Stempihar 2013).

Based on the literature, the guayule-based binder cannot be fully assessed without investigating its behavior in the binder–aggregate mixture. Therefore, this study aimed to evaluate the behavior of previously established guayule-based binders in the mixture by carrying out commonly used asphalt mixture tests. Five designated mixtures were selected to address the asphalt replacement by guayule resin (called guayule as well in this study) and CRM. The tests involved assessments of the major distresses encountering flexible pavement as follows: moisture susceptibility, rutting resistance, fatigue cracking resistance, and thermal cracking resistance. The modified Lottman test was used to evaluate moisture susceptibility. The rut test using asphalt pavement analyzer (APA) was used to assess rutting resistance. In addition, the HWT test was used to evaluate both moisture susceptibilities and rutting resistances at the same time. Fatigue cracking and thermal cracking resistances were evaluated by the fracture energy mechanism using the SCB and DCT tests. Therefore, the applicability of guayule resin in the flexible pavement mixture could be initiated. Subsequently, guayule-based mixtures' enhancements can be founded in the future.

Materials and Methods

Materials

Binders' Preparation

Based on previous studies by the same research group (Hemida and Abdelrahman 2019a, 2020a, b, 2021a), designated binders were selected to evaluate the performance of the guayule-based binder through the mixture. The designated binders were established based on the following material sources: asphalt from Philips 66 Company, IL, CRM from Liberty Tire Recycling, and guayule resin from Bridgestone Corp. The CRM was received in different gradations, but the CRM #30–40 (passed mesh #30 and retained on mesh #40) was used according to the US standard system (Ghavibazoo et al. 2013; Zaumanis et al. 2014). The designation implied five binders, which were neat asphalt (PG64-22), neat guayule (PG58-10), one asphalt–rubber–guayule blend [ARG (75-20)], and two guayule–rubber blends [GR(12.5), and GR(25)]. The ARG(75-20) binder included 75% asphalt rubber (20% rubber by weight of asphalt) plus 25% guayule. The GR(12.5) blend included a guayule–rubber binder (12.5% rubber by weight of blend). The GR(25) binder included a guayule–rubber blend (25% rubber by weight of blend). The Superpave performance grade of each designated binder is provided in Table 1.

Blending was carried out using a high shear mixer, temperature controller, and a heating mantle (Hemida and Abdelrahman 2019a, 2020b, 2021a, b). Before blending, guayule was heat-treated at a 160°C blending temperature with a 600-rpm rotational speed until no bubbling or foaming visually appeared to ensure that no moisture or low molecular weight components were involved (Hemida and Abdelrahman 2019a, 2020b, 2021a, b). The 160°C temperature represented an approximate temperature used in the flexible pavement construction process, which is simulated by 163°C in the laboratory short-term aging using the rolling thin film oven (RTFO). Therefore, the volatiles were minimized and guayule was ready to simulate the construction process. The 600-rpm rotational speed was assigned as a slow speed just for stirring to keep the material isothermal with no vortex formation. Rubber was oven-dried before any interaction with asphalt and/or guayule. As recommended in the literature, the blending technique was applied (Abdelrahman

Table 1. Binders' data

Binder	Code	Proportions			Superpave performance grade (°C)		
		A%	G%	CRM%	PG-HT	PG-IT	PG-LT
Neat asphalt	A	100	—	—	64	20	−22
Neat guayule	G	—	100	—	58	31	−10
Asphalt–rubber–guayule blend	ARG(75-20)	62.5	25	12.5	70	22	−16
Guayule–rubber blend (1)	GR(12.5)	—	87.5	12.5	58	34	−10
Guayule–rubber blend (2)	GR(25)	—	75	25	64	34	−4

Note: Superpave performance grades are listed based on the dynamic shear rheometer (DSR) and bending beam rheometer (BBR) measurements; PG-HT = performance grade high temperature; PG-IT = performance grade intermediate temperature; and PG-LT = performance grade low temperature.

et al. 2014; Ghavibazoo and Abdelrahman 2014; Ghavibazoo et al. 2016; Hemida and Abdelrahman 2019a). Regarding the preparation of the asphalt–rubber–guayule blend, first, the preheated asphalt was mixed with the oven-dried rubber for 40 min at 190°C and 3,000 rpm. Then, the preheated guayule was added, and the entire blend was mixed for 1 h at 160°C and 600 rpm. Considering the preparation of the guayule–rubber blend, the same process of the asphalt–rubber–guayule blend was followed except for the asphalt portion, which was replaced by guayule to end up with the same interaction parameters (speed, time, and temperature). In all interactions, no vortex formation was considered to minimize aging in either guayule's heat treatment process or materials' blending.

Aggregate Gradation

According to AASHTO M 323 (AASHTO 2017) and MoDOT 403 (MoDOT 2020), a job mix formula was followed to investigate the guayule-based binders in the field-simulated lab mixtures. Five individual aggregates were used to make an accepted aggregate blend with the MoDOT's Superpave mix design procedure. The five aggregate types and proportions were as follows: three Potosi Dolomite Formation (29% of 9/16 in. clean, 29% of 3/8 in. clean, and 15% of screenings), 25% of manufactured sand (crushed gravel), and 2% of mineral fillers (200 mesh). The aggregate blend had a 12.5-mm (1/2 in.) nominal maximum aggregate size, called SP125 in the Superpave mix design procedure. Fig. 1 illustrates the combined aggregate gradation, compared to the Superpave and MoDOT specification limits: Superpave upper and lower specification limits (USL and LSL, respectively) as well as MoDOT 403 SP125 USL and LSL.

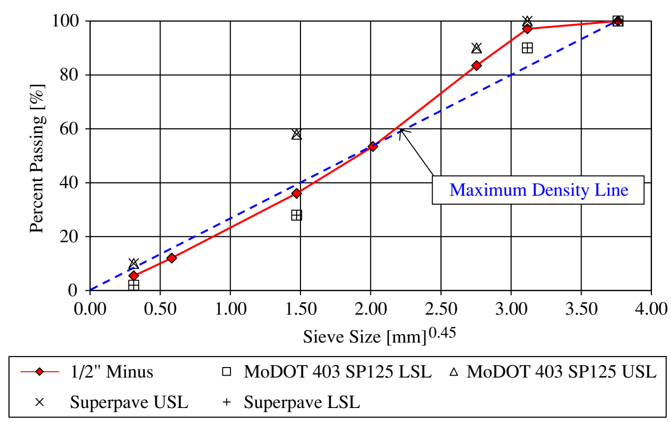

Fig. 1. Aggregate gradation.

Investigated Mixes

Fig. 2 shows the flowchart of the designated five mixtures for investigations. The five mixtures were determined to address the effect of the binder replacements on the mixture performance. Mixture IDs were defined in the footnote underneath the flowchart. The neat asphalt mixture (A-Mix) was selected to be compared with the asphalt–rubber–guayule mixture [ARG(75-20)-Mix]. Guayule was also investigated in mixtures as an entire asphalt cement alternative. Based on its performance limitations, a neat guayule mixture (G-Mix) was assessed. Fig. 3 shows the neat guayule mix as loose and compacted mixes. Two guayule–rubber mixtures were selected to analyze the performance changes by rubber addition in two different concentrations (12.5 and 25%, by weight of blend), named GR(12.5)-Mix and GR(25)-Mix, respectively.

To determine the air content (V_a) of each compacted mixture, the theoretical maximum specific gravity (G_{mm}) and bulk specific gravity (G_{mb}) were determined, according to AASHTO T 209 (AASHTO 2020b) and AASHTO T 166 (AASHTO 2020a), respectively. Table 2 illustrates the G_{mm} value of each designated mixture.

Methods

After considering the proper mixing and compaction requirements, the designated mixtures were exposed to common-used and advanced levels of mixture testing. The investigations involved assessments of moisture susceptibility, rutting resistance, fatigue cracking resistance, and thermal cracking resistance, which represented the major distresses according to the Superpave grading system. Recent versions of standards/specifications were followed. The designated mixtures were mainly made with respect to temperatures and air voids recommended throughout standards/specifications, thus assessing mixtures with respect to the critical end result parameters defined in literature and regardless of consistent testing temperature and/or air voids. In each test, sufficient replicates of each tested sample were applied for statistical considerations of averages [and coefficient of variations (COVs)], according to each standard/specification requirements, as well as excluding the outlier outcomes.

Mixing and Compaction Temperatures

A rotational viscometer was used to determine the five mixtures' mixing and compaction temperature ranges. Table 3 demonstrates the accepted temperature ranges according to viscosity

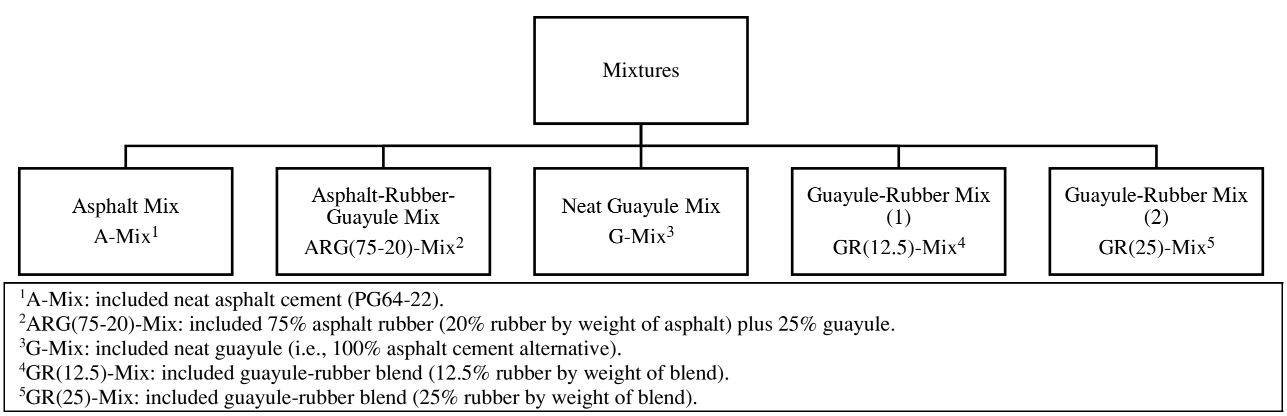

Fig. 2. Investigated mixtures.

Fig. 3. Neat guayule mixture (G-Mix): loose and compacted.

Table 2. G_{mm} values of designated mixtures

Designated mix	G_{mm} (unitless)
A-Mix	2.526
G-Mix	2.540
ARG(75-20)-Mix	2.549
GR(12.5)-Mix	2.550
GR(25)-Mix	2.546

Table 3. Mixing and compaction temperatures

	Temperature range (°C)	
Designated mix	Mixing	Compaction
A-Mix	152–158 (155)	135–143 (143)
G-Mix	141–146 (143)	121–127 (127)
ARG(75-20)-Mix	176–181 (176)	164–169 (165)
GR(12.5%)-Mix	146–153 (150)	132–138 (135)
GR(25%)-Mix	172–178 (176)	159–165 (165)

Note: The number between the two parentheses indicates the selected temperature for mixing or compaction.

values of 0.170 ± 0.020 Pa · s and 0.280 ± 0.030 Pa · s, respectively (Yildirim et al. 2000). The applied mixing and compaction temperatures are mentioned between the two parentheses.

Mixing and Compaction Processes

The individual aggregates were oven-dried until a constant mass was achieved, thus indicating no further moisture was inside, then they were combined. The mixing temperature was used for mixing pans, mixing paddles, combined aggregate, and asphalt binder. AASHTO R 30-02 (AASHTO 2019d) was followed to account for aging process. A mechanical mixer was used to prepare the loose mixtures. In this study, the designated mixtures were established according to the conventional asphalt mix design with respect to the Superpave mix design (the optimum asphalt content, $P_b = 4.7\%$). A Superpave gyratory compactor was used to prepare the Superpave mix cores, according to AASHTO T 312-19 (AASHTO 2019c), in which G_{mb} was determined based on each V_a requirement.

Mixture Tests

Mixture tests were selected to address the major distresses (rutting, fatigue cracking, and thermal cracking) in addition to moisture susceptibility evaluations. Fig. 4 illustrates the applied mixture tests in this study, as associated with the followed standards/specifications. Superpave recognized the modified Lottman test to assess moisture susceptibility. Therefore, it could be an initial indicator of applicability prediction for the guayule-based mixtures against moisture damage (stripping). Even though researchers used this standard method of moisture sensitivity assessment, it is not highly correlated to the field performance (Rafiq et al. 2020). The HWT test is not a standard method recognized by Superpave. Nevertheless, the HWT test could be a representative tool to evaluate the moisture susceptibility in addition to the associated rutting potential. The rut test by APA is a common technique directly relevant to the rutting resistance assessment used in this study. To predict cracking potential in the designated mixtures at intermediate and low temperatures, the concept of fracture energy was utilized. The SCB test was used to evaluate the fatigue cracking resistance at the intermediate temperature. The DCT test was used to assess the thermal cracking resistance at low temperatures. The DCT test is more reliable than the SCB tests regarding the thermal cracking assessment because of the long crack path that provides time to analyze the crack propagation at low temperatures (Radeef et al. 2021). However, the validity of the DCT test applications was only offered at low temperatures up to +10°C (ASTM 2020).

Moisture Susceptibility. The modified Lottman test is included in the Superpave Mix Design procedures (Roberts et al. 1996). In this study, AASHTO T 283 (AASHTO 2018) was followed to investigate the moisture susceptibility of all five designated mixtures. For each designated mixture, a minimum of six-core specimens were made with a 6.5%–7.5% V_a and divided into two sets (dry and wet). The first set involved three dry cores (control), and the other set involved three wet cores (conditioned); all were exposed to vacuum saturation of 70%–80% with water. The wet set was exposed to one freezing cycle for 16 h at −18°C and one thaw cycle in a 60°C water bath for 24 h. Afterward, both sets were conditioned in a 25°C water bath for 2 h before testing. The indirect tensile strength was measured using a load rate of 50.8 mm/min (2 in./min), and averages were calculated to acquire the tensile strength ratio (*TSR*), according to Eq. (1) (Roberts et al. 1996). Many agencies recommended the *TSR* to be no less than 70% (Roberts et al. 1996)

$$TSR = \frac{Indirect\,Tensile\,Strength\,of\,Conditioned\,set}{Indirect\,Tensile\,Strength\,of\,control\,set} \quad (1)$$

Rutting Susceptibility. The mixture's rutting susceptibility was investigated using the APA. The rut test was carried out according to AASHTO T 340-10 (AASHTO 2019b). A 64°C testing temperature

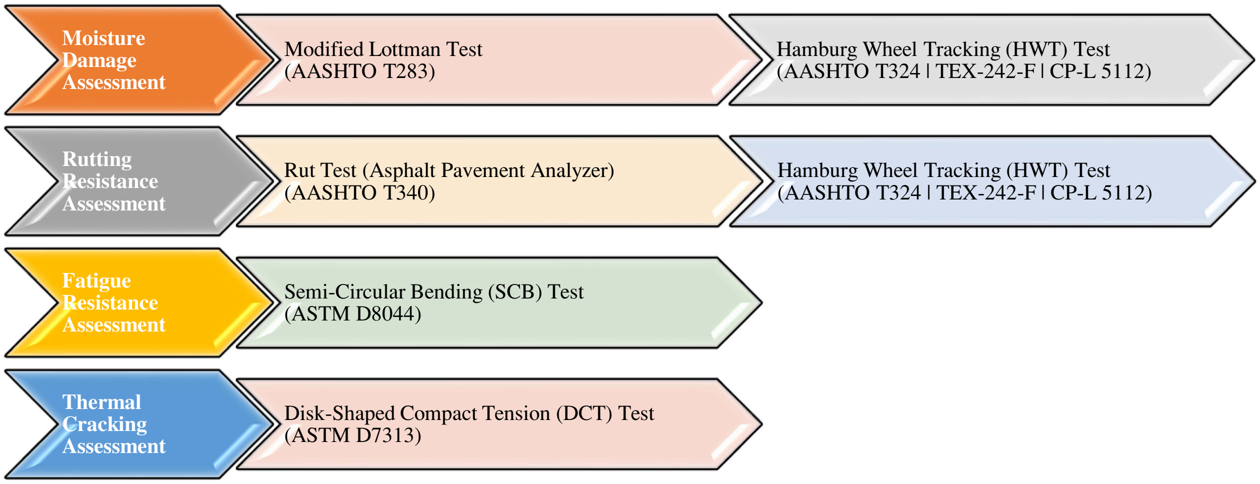

Fig. 4. Flowchart of mixture tests.

Fig. 5. Technical steps from the rut test procedures.

was selected to compare stiff mixtures [i.e., A-Mix, ARG(75-20)-Mix, and GR(25)-Mix]. A 58°C testing temperature was selected to compare soft mixtures [i.e., GR(12.5)-Mix and G-Mix]. Stiffer and softer mixtures were identified according to the binders' PG-HTs. The core samples—involving a V_a of 6.5%–7.5%—were installed in the molds and set in the APA chamber for 6 h before testing to ensure the isothermal condition. Eight thousand passes were applied based on 60 cycles/min at the test temperature. Fig. 5 shows technical steps from the rut test procedures conducted by the APA.

HWT. The HWT test was used to investigate moisture susceptibilities and rutting resistances of the designated mixtures using the modified APA. Moisture damage could occur for many reasons, such as cohesion failure induced by moisture (Rafiq et al. 2020). AASHTO T 324-19 reported that the testing temperature is specified by the agency (AASHTO 2019a). Colorado Department of Transportation (CDOT) Test Criteria (CP-L 5112) specified the test temperature based on the binder's PG-HT (i.e., 40°C for PG52, 45°C for PG58, 50°C for PG64, and 55°C for PG70 or higher) (Fitts 2005). The lab-compacted specimen is required to contain a $6\% \pm 2\%$ V_a. CDOT defined the failure when the rut depth went beyond 4 mm at 10,000 passes (CDOT 2020). Texas Department of Transportation (TxDOT), TEX-242-F, specified a constant temperature of 50±1°C regardless of the binder grade (TxDOT 2019). The lab-compacted specimen is required to contain a 7%±1% V_a. The test outcome is considered a failure if the rut depth is greater than 12.5 mm (Fitts 2005). TxDOT identified the minimum number of passes according to the binder grade (i.e., 10,000 passes for PG64 or lower, 15,000 passes for PG70, and 20,000 passes for PG76 or higher) (Fitts 2005). In this study, the HWT test was primarily carried out with monitoring the outcomes according to the two specifications. Fig. 6 shows technical steps from the HWT test procedures.

Fatigue Fracture Resistance. The concept of the SCB test was introduced by Mull et al. (2002) to evaluate asphalt mixtures involving CRM. Afterward, this concept was utilized to investigate fatigue fracture resistance of asphalt mixtures in Louisiana (Kim et al. 2012; Moore 2016). In this study, the five designated mixtures were analyzed using the SCB test at 25°C, which is highly recommended by the Louisiana Transportation Research Center (Cooper et al. 2016) and found suitable by several researchers to estimate the mixture's fatigue fracture resistance (Kim et al. 2012). The 25°C test temperature was used in literature to address the fatigue cracking resistance as a representative intermediate test temperature (Cooper et al. 2016; Kim et al. 2012; Moore 2016; VanFrank et al. 2017). At a rate of 0.5 mm/min, the three-point bending test was conducted, according to ASTM D8044 (ASTM 2016), in which the specimen represented a half-disk with a notch cut depth parallel to the loading and vertical axis. The specimen was loaded monotonically up to fracture failure occurrence (ASTM 2016; Kim et al. 2012). The applied contact load was 0.045 kN. The target V_a was 6.5%–7.5% (ASTM 2016). Louisiana Department of Transportation and Development (LADOTD) recommended three sets of specimens with notch depths of 25, 32, and 38 mm (ASTM 2016; Cooper et al. 2016; Kim et al. 2012; Moore 2016; VanFrank et al. 2017). Technical steps from the SCB test procedures are shown in Fig. 7. The critical strain energy release rate (*J-integral* or J_c) end result parameter, illustrated in Eq. (2), was utilized to evaluate the fatigue fracture resistance. The *J-integral* is a function

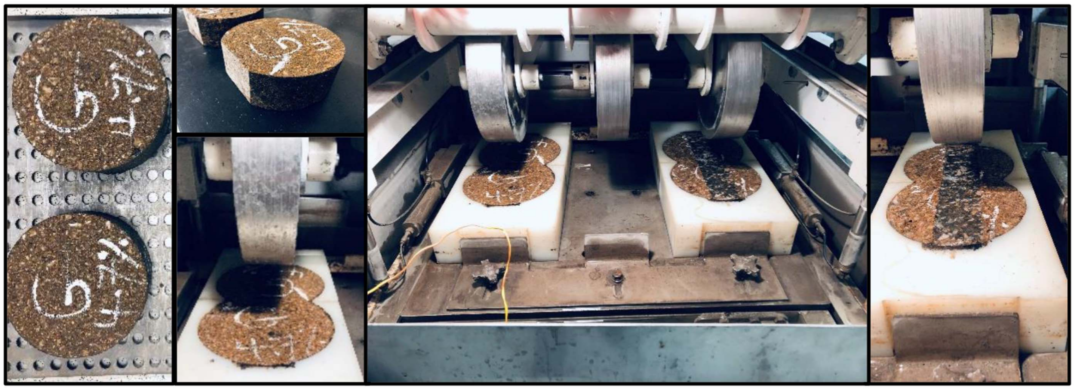

Fig. 6. Technical steps from the HWT test procedures.

Fig. 7. Technical steps from the SCB test procedures.

of the rate of change of strain energy per notch depth (dU/da) (Kim et al. 2012). Previous studies revealed that soft binders might reduce fracture resistance at intermediate temperatures (Cooper and Mohammad 2019; Cooper et al. 2016; Kim et al. 2012)

$$J_c = -\left(\frac{1}{b}\right)\frac{dU}{da} \quad (2)$$

where J_c is the critical strain energy release rate, kJ/m^2; b is the specimen thickness, mm; a is the notch depth, mm; U is the strain energy to failure (area under the load-displacement curve to peak load), N·mm; and dU/da is the change of strain energy with notch depth (strain energy–notch depth slope).

LADOTD recommended a minimum of 0.45 kJ/m^2 to indicate a threshold acceptance of a mixture's resistance to fatigue fracture cracking (Cooper et al. 2016). Studies reported that the higher the J_c value, the higher the fracture resistance to fatigue cracking (Bell 1990).

Low-Temperature Cracking. The DCT test was selected to investigate the fracture energy (G_f) at low temperatures, as illustrated in Eq. (3) (ASTM 2020), to evaluate the thermal fracture properties of the designated mixtures. Technical steps from the DCT test procedures are shown in Fig. 8. The target V_a was 6.5%–7.5%. Literature established that the quality of the DCT results decrease when temperatures increase beyond +10°C (ASTM 2020). Better DCT fracture energy outcomes were associated with soft binders at low temperatures (Buttlar et al. 2018; Zegeye et al. 2012). Based on the literature, the test temperature was selected at 10°C greater than the PG-LT (ASTM 2020; Johanneck et al. 2015). In addition to carrying out measurements at 10°C greater than the PG-LT, measurements at different low temperatures were taken to investigate further effects of low-temperature changes on designated mixtures. ASTM D7313 (ASTM 2020) was followed to conduct this test. A constant crack mouth opening displacement (CMOD) rate of 0.017 mm/s (approximately 1 mm/min) controlled the DCT test (ASTM 2020; Johanneck et al. 2015). The seating (contact) and post-peak loads were applied 0.1 kN. The specimen geometry was set with respect to ASTM D73-13 (ASTM 2020). Specimens were temperature-conditioned in the DCT instrument's environmental chamber for 2 h to ensure the isothermal condition (ASTM 2020)

$$G_f = \frac{Area}{B(W-a)} \quad (3)$$

where G_f is the fracture energy, J/m^2; $Area$ is the area under load-CMOD curve up to 100 N, N · m; B is the specimen thickness, m; and W-a is the ligament length, m.

Studies reported a threshold G_f value of 400 J/m^2 to indicate an acceptable threshold value of fracture energy to resist low-temperature

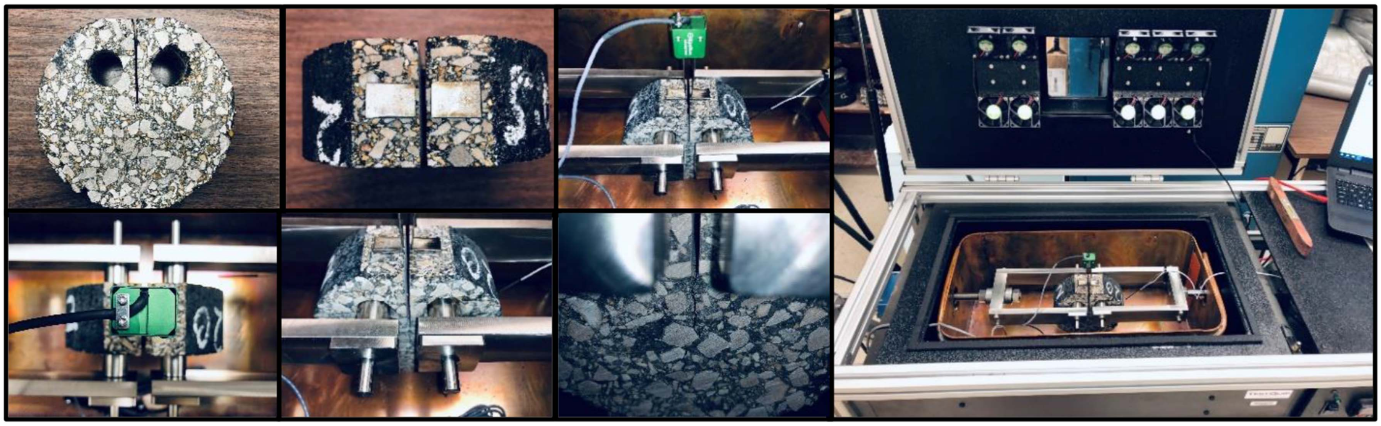

Fig. 8. Technical steps from the DCT test procedures.

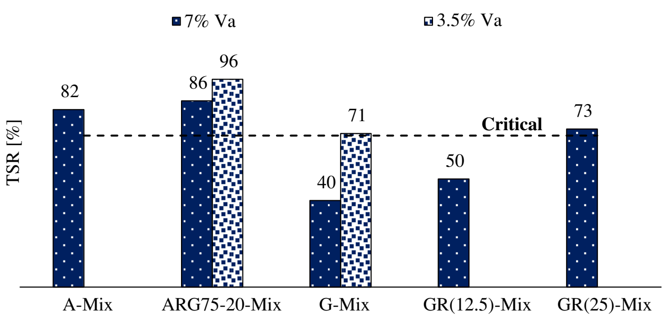

Fig. 9. Moisture susceptibility (TSR) results from the modified Lottman test.

cracking (Johanneck et al. 2015) to allow short-term aged specimens to be utilized (Buttlar et al. 2018).

Results and Discussion

Moisture Susceptibility

The results of the modified Lottman test was estimated based on (at least) six specimens in two subsets (dry and conditioned) for each designated mixture (AASHTO 2018). A subset of three dry specimens was used to calculate the average indirect tensile strength of the unconditioned (dry) specimens (AASHTO 2018). A subset of three conditioned specimens was used to calculate the

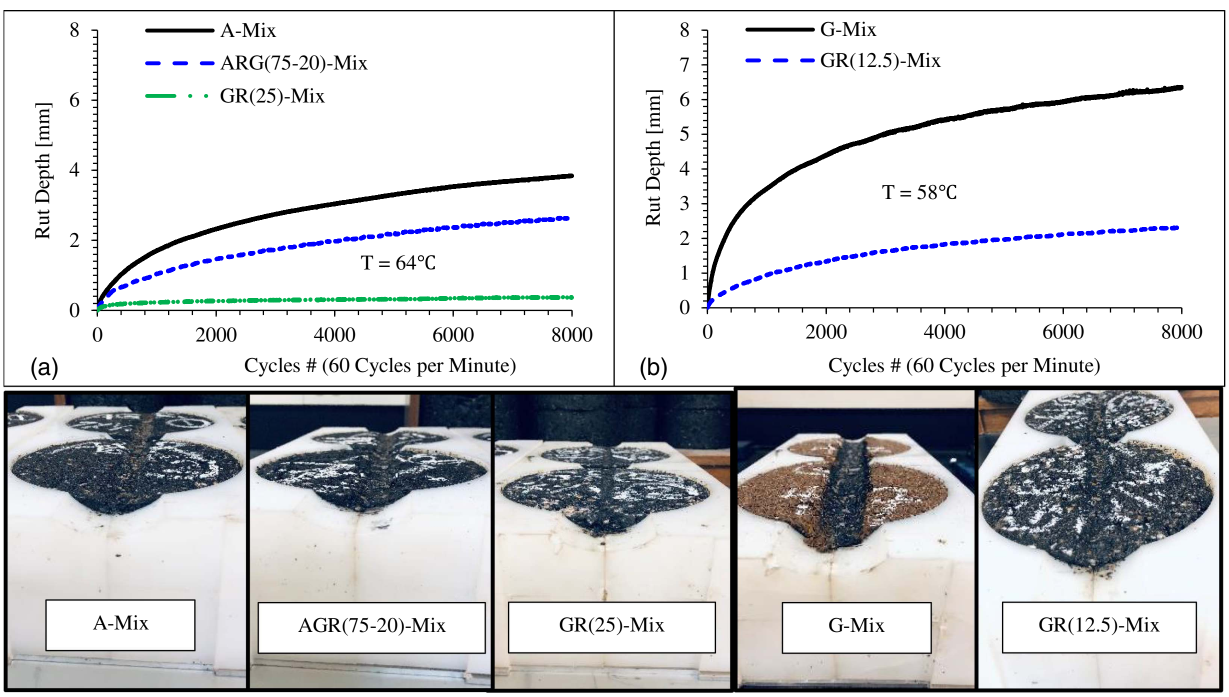

Fig. 10. Rut test results: (a) A-Mix, ARG(75-20)-Mix, and GR(25)-Mix at a 64°C test temperature; and (b) G-Mix and GR(12.5)-Mix at a 58°C test temperature; associated with the specimens' appearances after testing.

average indirect tensile strength of the conditioned specimens (AASHTO 2018). Outlier specimens were eliminated from the statistical considerations. Fig. 9 illustrates the *TSR* results. The G-Mix resulted in a dramatically low *TSR* (40%). In contrast, A-Mix resulted in an 82% *TSR* at the same mixture parameters, indicating potentially significant moisture damage to G-Mix at a 7% V_a level. Using guayule as a 100% asphalt alternative in the mixture would require mix parameter changes according to the standard modified Lottman test criteria, such as P_b, V_a, and/or antistripping agent addition parameters. For instance, changing V_a to 3.5% changed the *TSR* of G-Mix to 71%, indicating a significant moisture-resisting enhancement to the neat guayule mix. In addition, the CRM concentration gradually increased the moisture damage resistance. For instance, adding 20% CRM to guayule in GR(25)-mix changed the *TSR* from 40 to 73% at the same high V_a (7%). The ARG(75-20)-Mix provided enhanced *TSR* values at 7% V_a and 3.5% V_a (86 and 96%, respectively).

Rutting Susceptibility

The PG-HTs of A-Mix, ARG(75-20)-Mix, and GR(25)-Mix were 64°C, 70°C, and 64°C, respectively. Nevertheless, to compare the novel binders' behaviors in the mixture to the A-Mix, rut depths were addressed at a 64°C test temperature. On the other hand, G-Mix and GR(12.5)-Mix were tested at a 58°C test temperature because they had the same PG-HT (58°C).

The results of the rut test was estimated based on six specimens for each designated mixture (three pairs of wheel paths) (AASHTO 2019b). An average of the three pairs was considered (AASHTO 2019b). As shown in Fig. 10(a), the results showed that the rut depth trend was minor with GR(25)-Mix, followed by ARG(75-20)-Mix, then A-Mix. Compared to the measured binder performance at high temperatures, the rut test revealed that the GR(25)-Mix had a significantly lower rut depth (0.4 mm), thereby indicating that the GR(25)-mix could provide a high enhancement to the rutting resistance more than what was expected according to the Superpave criteria of the

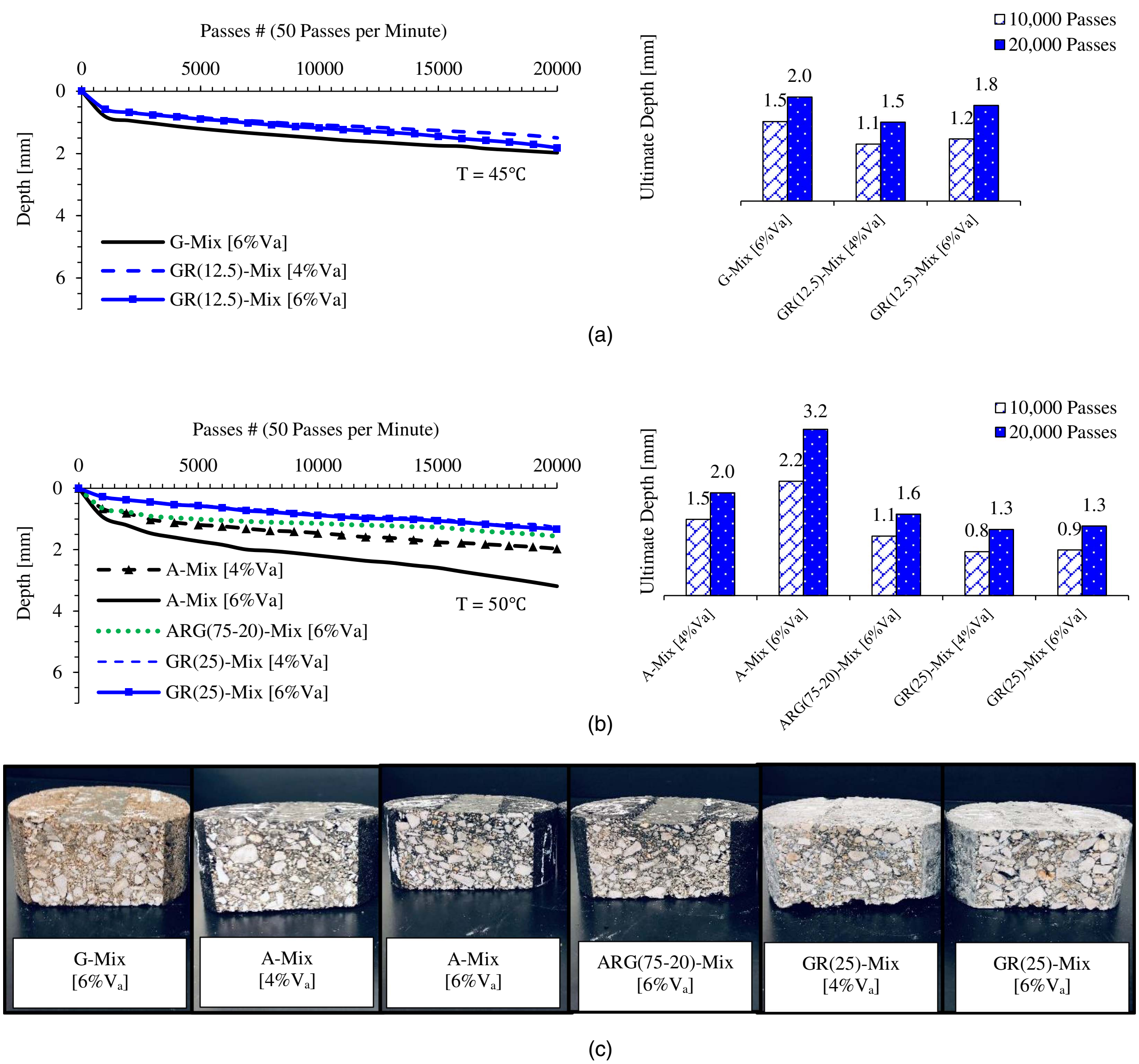

Fig. 11. HWT test results: (a) G-Mix and GR(12.5)-Mix at a 45°C test temperature; (b) A-Mix, ARG(75-20)-Mix and GR(25)-Mix at 50°C test temperature; and (c) some specimens' appearances after 20,000 passes.

binder performance. As expected, ARG(75-20)-Mix presented a better performance than that of A-Mix because ARG(75-20) had a 70°C PG-HT, and A-Mix had a 64°C PG-HT. Ultimately, the three mixtures provided undoubtedly excellent resistances to rutting.

As shown in Fig. 10(b), G-Mix presented an acceptable rut depth at a 58°C test temperature, which was compatible with the binder's rheological performance. The maximum rut depth associated reached 6.35 mm. At the same test temperature (58°C), GR (12.5)-Mix presented an enhanced rutting resistance (rut depth = 2.3 mm) compared to G-Mix, indicating the enhancement provided by the CRM to the neat guayule at high temperatures. In all studied cases, the rut depth went lower than the limits recommended by many DOTs (Fwa et al. 2012).

HWT

The results of the HWT test was estimated based on four specimens for each designated mixture (two pairs of wheel paths) (AASHTO 2019a). An average of the two pairs was considered (AASHTO 2019a). Fig. 11 illustrates the designated mixtures' performances using the HWT test. Most mixtures were tested at two different air contents as follows: 4% V_a and 6% V_a. Generally, all designated mixtures behaved perfectly despite their exposure to severe environmental and load parameters. In addition, the stripping inflection point was not reached for all designated mixtures, indicating no moisture damage (stripping) potential at this level of testing. Due to the aforementioned binder performance outcomes, G-Mix and GR(12.5)-Mix were tested at a 45°C test temperature, whereas A-Mix, ARG(75-20)-Mix, and GR(25)-Mix were tested at a 50°C test temperature. G-HMA exhibited an outstanding performance after 10,000 passes (in agreement with CP-L 5112) and after the extended 20,000 passes, as shown in Fig. 11(a). The rut depth decreased when modifying guayule by CRM in GR(12.5)-Mix. As expected, the evolution of V_a slightly increased the rut depth, as observed from the difference between GR(12.5)-Mix [4%V_a] and GR(12.5)-Mix [6%V_a].

At a 64°C test temperature, A-mix, ARG(75-20)-Mix, and GR (25)-Mix were HWT tested. These mixtures were not exposed to stripping at this level of testing because their stripping inflection points were not reached. Results revealed that all mixtures passed the HWT test with respect to all checked standards/specifications after either 10,000 or 20,000 passes, as shown in Fig. 11(b). Fig. 11(c) shows the appearance of some core specimens after HWT testing. When comparing A-Mix [4%V_a] to A-Mix [6%V_a], the rut depth noticeably changed due to the V_a parameter change. The GR(25)-Mix at the two levels of air contents (4 and 6%) resulted in slight changes in rut depths at 10,000 and 20,000 passes. The ARG(75-20)-mix presented an enhanced moisture resistance compared to A-Mix. Therefore, the three designated mixtures' performances against moisture damage were ranked in descending order as follows: GR(25)-Mix, ARG(75-20)-Mix, then A-Mix.

Mixture Performance at Intermediate Temperature

The results of the SCB test was estimated based on 12 specimens for each designated mixture (ASTM 2016). The strain energy–

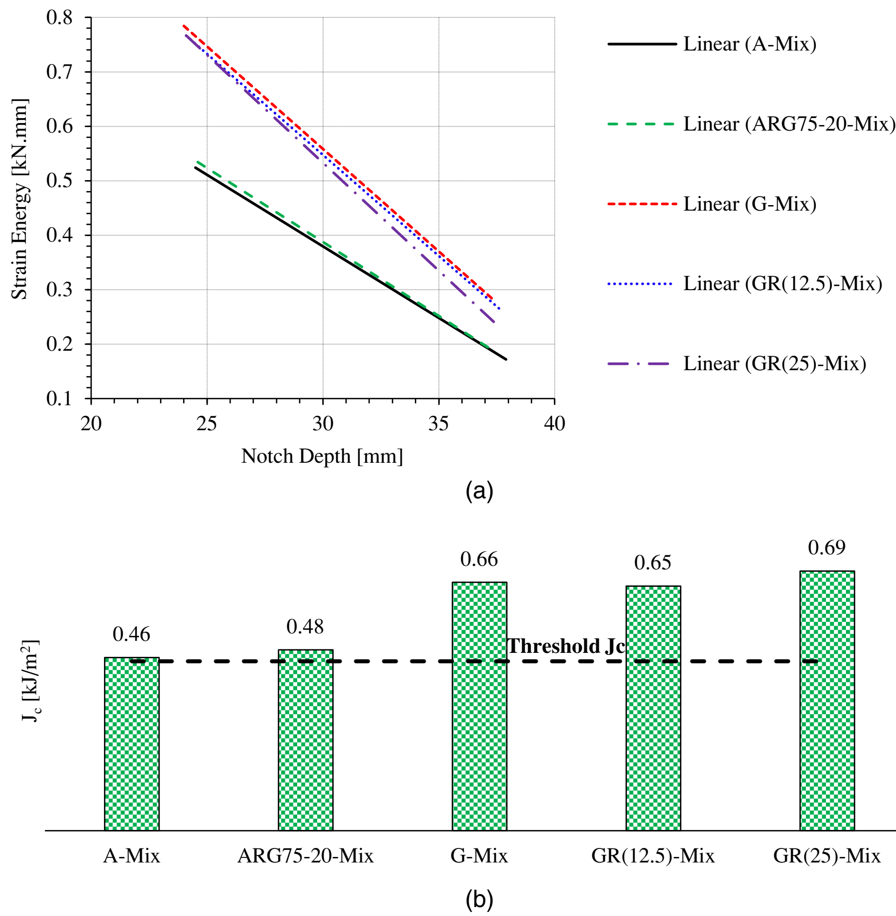

Fig. 12. SCB test results: (a) rate of change of strain energy per notch depth, strain energy–notch depth slope (dU/da); and (b) critical strain energy release rate (J_c).

notch depth slope of each designated mixture was illustrated based on four semicircular specimens at each notch depth (25, 32, and 38 mm). Outlier specimens were eliminated and COV of less than 9.9% was considered for this test's results (ASTM 2016). Fig. 12 illustrates the strain energy versus notch depth charts of the designated mixtures in linear regression to acquire the resultant slope (dU/da), and J_c values. The steeper the slope, the tougher the material (VanFrank et al. 2017). Fig. 12(a) demonstrates comparable A-Mix and ARG(75-20)-Mix slope values. Further, it demonstrates comparable G-Mix, GR(12.5)-Mix, and GR(25)-Mix slope values. In Fig. 12(b), the J_c of A-Mix resulted in 0.46 $\mathrm{kJ/m^2}$. This value was considered the control J_c value to assess the novel guayule-based mixtures. The asphalt–rubber–guayule mixture (ARG(75-20)-Mix) yielded a J_c value of 0.48 $\mathrm{kJ/m^2}$. This value indicated the predicted applicability or harmony among asphalt, rubber, and guayule in the mix performance against fatigue fracture resistance. In addition, this application explained the excessive compensation of conventional asphalt performance by rubber and guayule at the level of testing and material parameters. The neat guayule mix (G-Mix) yielded a J_c value of 0.66 $\mathrm{kJ/m^2}$, which contrasted with the binder's intermediate-temperature performance assessment, but it was in agreement with the SCB testing background (Cooper and Mohammad 2019; Cooper et al. 2016; Kim et al. 2012). The neat asphalt binder presented a better performance at intermediate temperatures (i.e., the neat asphalt possessed a lower PG-IT) than the neat guayule. The $0.66-\mathrm{kJ/m^2}J_c$ value demonstrated G-Mix's high fatigue fracture resistance compared to A-Mix, which was better than expected. The guayule–rubber mixtures produced comparable mix performances to the G-Mix against fatigue fracture, 0.65 $\mathrm{kJ/m^2}$ for GR(12.5)-Mix and 0.69 $\mathrm{kJ/m^2}$ for GR(25)-Mix. This could be an initial indication of the effect of rubber concentration increase/decrease on the fatigue fracture resistance of guayule–rubber mixtures.

The positive impact of the guayule-based binders in mixtures regarding the fracture resistance reflected the great fracture toughness of partial or entire asphalt cement replacement by guayule. Guayule presented a better performance in the mixture than the neat asphalt. The reason for that might be the ignorance of fracture toughness assessment for binders. The guayule-based mixture offered a steeper absolute value of the slope (dU/da) (i.e., a higher rate of change of strain energy per notch depth, which indicated a tougher material at this level of testing) compared to that of the asphalt-based mixture (VanFrank et al. 2017).

Mixture Performance at Low Temperature

The results of the DCT test was estimated based on an average of three specimens for each designated mixture (Radeef et al. 2021). Outlier specimens were eliminated and a G_fCOV of less than 15% was considered for each designated mixture (ASTM 2020; Radeef et al. 2021). Fig. 13(a) shows an example of a G-Mix specimen before and after the DCT test. Fig. 13(b) illustrates the fracture

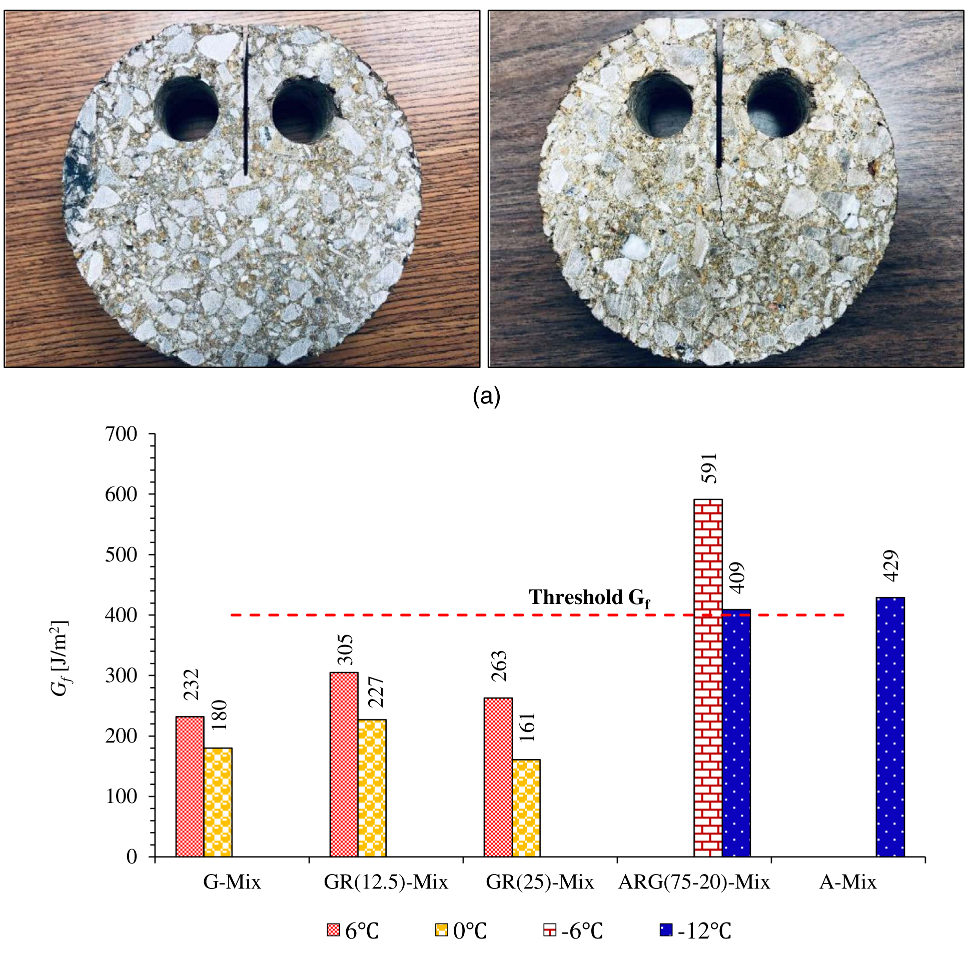

Fig. 13. DCT test: (a) example of a G-Mix before and after fracture; and (b) fracture energy (G_f) results.

Table 4. Summary table

Test	Mixture	T	V_a	End result parameter
Modified Lottman test	A-Mix	25°C	7% ± 0.5%	*TSR*: 82%
			3.5%	*TSR*: *N/A*
	G-Mix		7% ± 0.5%	*TSR*: 40%
			3.5%	*TSR*: 71%
	ARG(75-20)-Mix		7% ± 0.5%	*TSR*: 86%
			3.5%	*TSR*: 96%
	GR(12.5)-Mix		7% ± 0.5%	*TSR*: 50%
			3.5%	*TSR*: *N/A*
	GR(25)-Mix		7% ± 0.5%	*TSR*: 73%
			3.5%	*TSR*: *N/A*
Rut test (APA)	A-Mix	64°C	7% ± 0.5%	*RD*: 3.8 mm
	G-Mix	58°C		*RD*: 6.3 mm
	ARG(75-20)-Mix	64°C		*RD*: 2.6 mm
	GR(12.5)-Mix	58°C		*RD*: 2.3 mm
	GR(25)-Mix	64°C		*RD*: 0.4 mm
HWT test	A-Mix	50°C	4%	*RD*: 1.5 mm at 10,000 passes
				RD: 2 mm at 20,000 passes
			6%	*RD*: 2.2 mm at 10,000 passes
				RD: 3.2 mm at 20,000 passes
	G-Mix	45°C	4%	*RD*: *N/A* at 10,000 passes
				RD: *N/A* at 20,000 passes
			6%	*RD*: 1.5 mm at 10,000 passes
				RD: 2 mm at 20,000 passes
	ARG(75-20)-Mix	50°C	4%	*RD*: *N/A* at 10,000 passes
				RD: *N/A* at 20,000 passes
			6%	*RD*: 1.1 mm at 10,000 passes
				RD: 1.6 mm at 20,000 passes
	GR(12.5)-Mix	45°C	4%	*RD*: 1.1 mm at 10,000 passes
				RD: 1.5 mm at 20,000 passes
			6%	*RD*: 1.2 mm at 10,000 passes
				RD: 1.8 mm at 20,000 passes
	GR(25)-Mix	50°C	4%	*RD*: 0.8 mm at 10,000 passes
				RD: 1.3 mm at 20,000 passes
			6%	*RD*: 0.9 mm at 10,000 passes
				RD: 1.3 mm at 20,000 passes
SCB test	A-Mix	25°C	7% ± 0.5%	J_c:0.46 kJ/m^2
	G-Mix			J_c:0.66 kJ/m^2
	ARG(75-20)-Mix			J_c:0.48 kJ/m^2
	GR(12.5)-Mix			J_c:0.65 kJ/m^2
	GR(25)-Mix			J_c:0.69 kJ/m^2
DCT Test	A-Mix	6°C	7% ± 0.5%	G_f: *N/A*
		0°C		G_f: *N/A*
		−6°C		G_f: *N/A*
		−12°C		G_f:429 J/m^2
	G-Mix	6°C		G_f:232 J/m^2
		0°C		G_f:180 J/m^2
		−6°C		G_f: *N/A*
		−12°C		G_f: *N/A*
	ARG(75-20)-Mix	6°C		G_f: *N/A*
		0°C		G_f: *N/A*
		−6°C		G_f:591 J/m^2
		−12°C		G_f:409 J/m^2
	GR(12.5)-Mix	6°C		G_f:305 J/m^2
		0°C		G_f:227 J/m^2
		−6°C		G_f: *N/A*
		−12°C		G_f: *N/A*
	GR(25)-Mix	6°C		G_f:263 J/m^2
		0°C		G_f:161 J/m^2
		−6°C		G_f: *N/A*
		−12°C		G_f: *N/A*

Note: *N/A* = not available; *RD* = rut depth; T = test temperature; and V_a = air content.

energy (G_f) of the designated mixtures at 10°C greater than the PG-LT. Mixtures were exposed to other low temperatures to monitor the differences in their behaviors. Results showed that the A-Mix yielded a G_f value of 429 J/m^2 at a −12°C test temperature, which passed the threshold value established in literature, 400 J/m^2 (Johanneck et al. 2015). The neat guayule mixture or its modification by rubber did not improve the low-temperature cracking resistance. According to the Superpave criteria, binder investigations revealed the destructive behaviors of guayule binders at low temperatures, but not to the extent shown by the mixture outcomes. The threshold G_f value (400 J/m^2) was not reached for any of G-Mix, GR(12.5)-Mix, or GR(25)-Mix at 6°C or 0°C test temperatures. This could indicate the difficulty of using guayule (as a 100% asphalt alternative) with or without CRM, regarding material and interaction parameters, to resist the potential thermal cracking, indicating a worse low-temperature performance than what was predicted by the binder investigations.

The ARG(75-20)-Mix, which had a PG-LT of −16°C, remarkably provided an excellent fracture resistance at the corresponding test temperature (−6°C), 591 J/m^2. That was why the same mixture was exposed to −12°C to monitor its performance at that low test temperature. The results of ARG(75-20)-Mix positively ended with a G_f value of 409 J/m^2, indicating a potentially accepted mixture at a PG-LT of −22°C.

Summary

In Table 4, a summary of the major data acquired through this study was reported to summarize the input parameters (test temperature and air content) and end result parameters [*TSR*, rut depth (by APA), HWT rut depth, J_c, and G_f].

Conclusion

This study provided an evaluation of the innovative guayule bio-based mixtures against major distresses from the perspective of the binder–aggregate mixture: moisture damage, rutting, fatigue cracking, and thermal cracking. The following observations were made:

1. Guayule was worse than asphalt at resisting moisture damage through the standard modified Lottman test. By contrast, guayule-based mixtures presented a high resistance to moisture damage evaluated by the HWT test, and it was more reliable to address the field performance.
2. Neat guayule mixture had a high resistance to rutting at its high-temperature performance grade. Guayule modification using CRM and partial asphalt replacement by guayule and rubber enhanced the rutting resistance. This was compatible with the binder performance evaluated by the Superpave criteria.
3. Changing parameters (e.g., air content, rubber addition, and partial asphalt replacement by guayule and rubber) enhanced the guayule-based mixture's resistance to rutting and moisture damage resulting in acceptable performances by TSR, rut, and HWT tests.
4. The positive impacts of the guayule-based binders in mixtures regarding the fracture resistance at the intermediate temperature reflected the great fracture toughness of partial or entire asphalt replacement by guayule. Guayule offered better performance in the mixture than the neat asphalt due to the unavailability of the fracture toughness criterion in binder evaluation by the Superpave criteria. Compared to neat asphalt mixture, guayule-based mixture presented a higher rate of change of strain energy per notch depth, which indicated a tougher material.
5. Guayule (with or without CRM addition) did not offer the desired performance at low temperatures. This could indicate the difficulty of using guayule (as a 100% asphalt alternative) to resist the potential thermal cracking, thus indicating a worse low-temperature performance than expected from the Superpave's binder evaluation criteria. However, partial asphalt replacement by guayule and CRM resisted the thermal fracture greatly.
6. Future work is recommended to enhance the performance of the guayule-based mixtures, particularly at low temperatures. The rejuvenators' additions are potential material parameters that could significantly improve a mixture's performance at low and intermediate temperatures.

Data Availability Statement

All data, models, and code generated or used during the study appear in the published paper.

Acknowledgments

Special thanks go to Steven Lusher, Ph.D., for his assistance with providing technical support, materials, and information based on his experience with guayule. Likewise, the authors are grateful to the Bridgestone Corporation for creating guayule resin and providing valuable information in this regard.

Notation

The following symbols are used in this paper:

$Area$ = area under load-CMOD curve up to 100 N;
a = semicircular specimen notch depth;
B = disk specimen thickness;
b = semicircular specimen thickness;
dU/da = change of strain energy with notch depth (strain energy–notch depth slope);
G_f = fracture energy;
G_{mb} = bulk specific gravity;
G_{mm} = theoretical maximum specific gravity;
J_c = critical strain energy release rate;
P_b = binder content;
RD = rut depth;
T = test temperature;
TSR = tensile strength ratio;
U = strain energy to failure (area under the load-displacement curve to peak load);
V_a = air content; and
W-a = disk specimen ligament length.

References

AASHTO. 2017. *Standard specification for Superpave volumetric mix design*. AASHTO M 323-17. Washington, DC: AASHTO.

AASHTO. 2018. *Standard method of test for resistance of compacted asphalt mixtures to moisture-induced damage*. AASHTO T 283-14. Washington, DC: AASHTO.

AASHTO. 2019a. *Hamburg wheel-track testing of compacted hot mix asphalt (HMA)*. AASHTO T 324-19. Washington, DC: AASHTO.

AASHTO. 2019b. *Standard method of test for determining rutting susceptibility of hot mix asphalt (HMA) using the asphalt pavement analyzer (APA)*. AASHTO T 340-10. Washington, DC: AASHTO.

AASHTO. 2019c. *Standard method of test for preparing and determining the density of asphalt mixture specimens by means of the Superpave gyratory compactor*. AASHTO T 312-19. Washington, DC: AASHTO.

AASHTO. 2019d. *Standard practice for mixture conditioning of hot mix asphalt (HMA)*. AASHTO R 30-02. Washington, DC: AASHTO.

AASHTO. 2020a. *Standard method of test for bulk specific gravity (*Gmb*) of compacted asphalt mixtures using saturated surface-dry specimens*. AASHTO T 166-16. Washington, DC: AASHTO.

AASHTO. 2020b. *Standard method of test for theoretical maximum specific gravity (G mm) and density of asphalt mixtures*. AASHTO T 209-20. Washington, DC: AASHTO.

Abdelrahman, M., D. R. Katti, A. Ghavibazoo, H. B. Upadhyay, and K. S. Katti. 2014. "Engineering physical properties of asphalt binders through nanoclay–asphalt interactions." *J. Mater. Civ. Eng.* 26 (12): 04014099. https://doi.org/10.1061/(ASCE)MT.1943-5533.0001017.

Ahmad, M., B. K. Bairgi, Z. H. Khan, and R. A. Tarefder. 2020. "Evaluation of the fracture resistance of asphalt concrete mixes including the effect of anisotropy." *Int. J. Pavement Res. Technol.* 13 (2): 121–128. https://doi.org/10.1007/s42947-019-0092-2.

ASTM. 2016. *Standard test method for evaluation of asphalt mixture cracking resistance using the semi-circular bend test (SCB) at intermediate temperatures*. ASTM D8044-16. West Conshohocken, PA: ASTM International.

ASTM. 2020. *Standard test method for determining fracture energy of asphalt mixtures using the disk-shaped compact tension geometry.* ASTM D7313-20. West Conshohocken, PA: ASTM International.

Bell, C. 1990. "Relationship between laboratory aging tests and field performance of asphalt-concrete mixtures." In *Serviceability and durability of construction materials*, 745–754. New York: ASCE.

Buttlar, W., P. Rath, H. Majidifard, E. V. Dave, and H. Wang. 2018. "Relating DC (T) fracture energy to field cracking observations and recommended specification thresholds for performance-engineered mix design." *Transp. Res. Circ*. (E-C251): 51–71.

CDOT (Colorado DOT). 2020. *Standard method of test for Hamburg wheel-track testing of compacted bituminous mixtures*. CPL 5112-20. Denver: CDOT.

Cooper, S. B., W. King, and S. Kabir. 2016. *Testing and analysis of LWT and SCB properties of asphalt concrete mixtures*. Baton Rouge, LA: Louisiana Transportation Research Center.

Cooper, S. B., III, and L. N. Mohammad. 2019. "Implementation of balanced mixture criteria during asphalt mixture design: Louisiana's experience." *Transp. Res. Circ*. (E-C251): 22–30.

Deef-Allah, E., M. Abdelrahman, and A. Hemida. 2020. "Improving asphalt binder's elasticity through controlling the interaction parameters between CRM and asphalt binder." *Adv. Civ. Eng. Mater.* 9 (1): 262–282. https://doi.org/10.1520/ACEM20190204.

FHWA. 2013. "FHWA-HIF-13-005, Asphalt mixture performance tester (AMPT)." Accessed July 27, 2021. https://www.fhwa.dot.gov/pavement/asphalt/pubs/hif13005.pdf.

Fitts, G. L. 2005. "Hamburg wheel tracking (HWT) test." Accessed July 27, 2021. https://www.ltrc.lsu.edu/asphalt/pdf/Hamburg%20Wheel%20Tracking%20Test.pdf.

Fwa, T., H. Pasindu, and G. Ong. 2012. "Critical rut depth for pavement maintenance based on vehicle skidding and hydroplaning consideration." *J. Transp. Eng.* 138 (4): 423–429. https://doi.org/10.1061/(ASCE)TE.1943-5436.0000336.

Ghavibazoo, A., and M. Abdelrahman. 2014. "Effect of crumb rubber dissolution on low-temperature performance and aging of asphalt–rubber binder." *Transp. Res. Rec.* 2445 (1): 47–55. https://doi.org/10.3141/2445-06.

Ghavibazoo, A., M. Abdelrahman, and M. Ragab. 2013. "Effect of crumb rubber modifier dissolution on storage stability of crumb rubber–modified asphalt." *Transp. Res. Rec.* 2370 (1): 109–115. https://doi.org/10.3141/2370-14.

Ghavibazoo, A., M. Abdelrahman, and M. Ragab. 2016. "Changes in composition and molecular structure of asphalt in mixing with crumb rubber modifier." *Road Mater. Pavement Des.* 17 (4): 906–919. https://doi.org/10.1080/14680629.2016.1138878.

Hemida, A., and M. Abdelrahman. 2018. "A threshold to utilize guayule resin as a new binder in flexible pavement industry." *Int. J. Eng. Res. Appl.* 8 (12): 83–94.

Hemida, A., and M. Abdelrahman. 2019a. "Influence of guayule resin as a bio-based additive on asphalt–rubber binder at elevated temperatures." *Recycling* 4 (3): 38. https://doi.org/10.3390/recycling4030038.

Hemida, A., and M. Abdelrahman. 2019b. "Review on rheological characterization of bio-oils/bio-binders and their applicability in the flexible pavement industry." *Int. J. Civ. Eng. Technol.* 10 (12): 395–405. https://doi.org/10.17605/OSF.IO/4Q6CR.

Hemida, A., and M. Abdelrahman. 2020a. "Effect of guayule resin as a bio-based additive on storage stability and liquid phase separation of asphalt rubber binder." In *Proc., 99th Annual Meeting of the Transportation Research Board*. Washington, DC: Transportation Research Board.

Hemida, A., and M. Abdelrahman. 2020b. "Monitoring separation tendency of partial asphalt replacement by crumb rubber modifier and guayule resin." *Constr. Build. Mater.* 251 (Aug): 118967. https://doi.org/10.1016/j.conbuildmat.2020.118967.

Hemida, A., and M. Abdelrahman. 2021a. "Component analysis of bio-asphalt binder using crumb rubber modifier and guayule resin as an innovative asphalt replacer." *Resour. Conserv. Recycl.* 169 (Jun): 105486. https://doi.org/10.1016/j.resconrec.2021.105486.

Hemida, A., and M. Abdelrahman. 2021b. "Guayule resin: An innovative bioresource for asphalt cement replacement." *J. Cleaner Prod.* 314 (Sep): 128065. https://doi.org/10.1016/j.jclepro.2021.128065.

Hemida, A., and M. Abdelrahman. 2021c. "Rheological and component characterization of an innovative bio-binder using guayule resin in partial and entire asphalt replacement." In *Proc., 99th Annual Meeting of the Transportation Research Board*. Washington, DC: Transportation Research Board.

Johanneck, L., J. Geib, D. Van Deusen, J. Garrity, C. Hanson, and E. V. Dave. 2015. *DCT low temperature fracture testing pilot project*. St. Paul, MN: MnDOT Library.

Kim, M., L. N. Mohammad, and M. A. Elseifi. 2012. "Characterization of fracture properties of asphalt mixtures as measured by semicircular bend test and indirect tension test." *Transp. Res. Rec.* 2296 (1): 115–124. https://doi.org/10.3141/2296-12.

MoDOT. 2020. *Missouri standard specifications for highway construction, Section 403 asphaltic concrete pavement*. Jefferson City, MO: MoDOT.

Moore, N. 2016. *Evaluation of laboratory cracking tests related to top-down cracking in asphalt pavements*. Auburn, AL: Auburn Univ.

Mull, M., K. Stuart, and A. Yehia. 2002. "Fracture resistance characterization of chemically modified crumb rubber asphalt pavement." *J. Mater. Sci.* 37 (3): 557–566. https://doi.org/10.1023/A:1013721708572.

Nakayama, F. 2005. "Guayule future development." *Ind. Crops Prod.* 22 (1): 3–13. https://doi.org/10.1016/j.indcrop.2004.05.006.

Radeef, H., N. A. Hassan, A. Z. Abidin, M. Mahmud, M. M. Satar, M. M. Warid, and Z. Al Saffar. 2021. "Determining fracture energy in asphalt mixture: A review." *IOP Conf. Ser.: Earth Environ. Sci.* 682 (1): 012069. https://doi.org/10.1088/1755-1315/682/1/012069.

Rafiq, W., M. Bin Napiah, M. Hartadi Sutanto, W. Salah Alaloul, Z. Nadia Binti Zabri, M. Imran Khan, and M. Ali Musarat. 2020. "Investigation on Hamburg wheel-tracking device stripping performance properties of recycled hot-mix asphalt mixtures." *Materials* 13 (21): 4704. https://doi.org/10.3390/ma13214704.

Rasutis, D., K. Soratana, C. McMahan, and A. E. Landis. 2015. "A sustainability review of domestic rubber from the guayule plant." *Ind. Crops Prod.* 70 (Aug): 383–394. https://doi.org/10.1016/j.indcrop.2015.03.042.

Roberts, F., P. Kandhal, E. Brown, D. Lee, and T. Kennedy. 1996. *Hot mix asphalt materials, mixture design and construction*. Greenbelt, MD: National Asphalt Pavement.

Stempihar, J. 2013. *Development of the C* fracture test for asphalt concrete mixtures*. Tempe, AZ: Arizona State Univ.

Stewart, C. M., J. G. Reyes, and V. M. Garcia. 2017. "Comparison of fracture test standards for a super pave dense-graded hot mix asphalt." *Eng. Fract. Mech.* 169 (Jan): 262–275. https://doi.org/10.1016/j.engfracmech.2016.10.016.

TxDOT (Texas DOT). 2019. *Test procedure for Hamburg wheel-tracking test*. Tex-242-F. Austin, TX: TxDOT.

VanFrank, K., M. VanMilligen, and T. Biel. 2017. *Intermediate temperature cracking in HMA: Phase 1 semi-circular bending (SCB) practicality evaluation*. Taylorsville, UT: Research Division, Utah DOT.

Yildirim, Y., M. Solaimanian, and T. W. Kennedy. 2000. *Mixing and compaction temperatures for hot mix asphalt concrete*. Austin, TX: Center for Transportation Research, Univ. of Texas at Austin.

Zaumanis, M., R. B. Mallick, and R. Frank. 2014. "100% recycled hot mix asphalt: A review and analysis." *Resour. Conserv. Recycl.* 92 (Nov): 230–245. https://doi.org/10.1016/j.resconrec.2014.07.007.

Zegeye, E. T., K. H. Moon, M. Turos, T. R. Clyne, and M. O. Marasteanu. 2012. "Low temperature fracture properties of polyphosphoric acid modified asphalt mixtures." *J. Mater. Civ. Eng.* 24 (8): 1089–1096. https://doi.org/10.1061/(ASCE)MT.1943-5533.0000488.